TBK-1-DC VACCINE INDUCES POLYFUNCTIONAL T CELLS AND CONTROL OF HIV-1 IN THE BLT MOUSE

Calvet-Mirabent M[1,2], Deruaz M[3], Tanno S[3], Delgado-Arévalo C[1,2], Sánchez-Cerrillo I[1], Serra C[5], Buzón MJ[5], de los Santos I[1], Sanz J[1], García-Fraile L[1], Muñoz-Fernández MA[4], Balazs A[3], Vrbanac V[3], Martín-Gayo E[1,2]

[1]Hospital Universitario de La Princesa, [2]Universidad Autónoma de Madrid, [3]Ragon Institute of MGH, MIT and Harvard and human Immune System core from Massachusetts General Hospital, Boston, MA; [4]Hospital Gregorio Marañón; [5]Infectious Diseases Department, Hospital Universitari Vall d'Hebron, Institut de Recerca (VHIR), Universitat Autònoma de Barcelona, Barcelona, Spain.

Poster #: 0295

Introduction

Dendritic cells (DC) are critical to induce protective antiviral T cell responses. Failure of previous HIV-1 vaccines suggests that further fine-tuning of DC function is essential for boosting HIV-1 specific immunity. TANK-binding Kinase 1 (TBK-1) is a key regulator required for maturation of DC in response to HIV-1 and to prime polyfunctional specific T cells linked to viral control. Our objective is to evaluate the efficacy of a vaccine based on TBK1-engineered DCs controlling HIV-1 infection *in vivo* using the humanized bone marrow, liver and thymus (hBLT) mouse model.

Hypothesis

DCs activated via TBK-1 adjuvants will be able to prime protective polyfunctional T cell responses against HIV-1 *in vivo* in the humanized mouse model.

Materials and methods

DC Vaccination and HIV-1 infection of hBLT mice: A total of 24 hBLT-mice were generated from NOD/SCID/IL2Rγc-deficient (NSG) mice transplanted with human fetal thymus, liver and CD34+ hematopoietic stem cells (HSC). DC were differentiated from autologous HSCs in the presence of FLT3L, IL-7, SCF and GMCSF. Three separate groups of 8 hBLT-mice were injected with HSC-derived DCs cultured in media (MED), gag peptides alone (GAG) or in combination with 2´-3´-c-AMP and Poly-I:C TBK-1 adjuvants (ADJ) and were subsequently infected intravenously with 10,000 TCID50 of JRCSF HIV-1 after 2 weeks. Plasma HIV-1 viral loads were assessed at 3 and 6 weeks post-infection. CD4+ T cell counts in blood and polyfunctional profiles of splenic T cells were also determined at 5 and 6 weeks post-infection (**Figure 1**).

Polyfunctional T cell response analysis: Polyfunctional cytokine responses in circulating CD8+ and CD4+ T cells from vaccinated hBLT mice were addressed at 3 and 6 week p.i. by multicolor flow cytometry after culture of PBMCs for 5h in the presence of media alone or containing a pool of HIV-1 gag peptides (NIH-reagent program) and supplemented with aCD49d, aCD28 and aCD107a mAbs and brefeldin-A. Polyfunctional profile from T cells resident in the spleen were also included at 6 weeks p.i. following the same protocol. Polyfunctionality was evaluated using Boolean gating obtained with FlowJo and analyzed with SPICE softwares.

Immunohistochemistry: Sections of spleen and Lymph nodes (LN) from hBLT mice at 6 weeks p.i. were embedded in paraffin and tissue sections were subsequently stained with DAPI, rabbit anti-human CD8 and mouse anti-HIV-1 p24 and rat anti-human Granzyme B primary monoclonal Abs and revealed with goat anti-rabbit Alexa F488, donkey anti-mouse Alexa F647 and donkey anti-rat Alexa F547 secondary Abs, respectively. Stacked immunofluorescence images were obtained by confocal microscopy. Quantification of CD8+ T cell, granzyme B+ cells and co-localization of both markers was calculated using Image J software. Quantification of CD8+ T cell aggregation volume in LNs was performed using the Imaris software. Relative distance of individuals p24+ cells to CD8+ T cells was calculated using the Image J software.

Results

▪All groups of hBLT-mice became infected with HIV-1, however animals vaccinated with autologous GAG-ADJ DCs exhibited a partial but significant reduction of HIV-1 plasma viral loads at 3 weeks p.i. compared to control groups. At 6 weeks post-vaccination, plasma viral loads were similar across different groups of vaccinated mice (**Figure 2**).

Figure 1

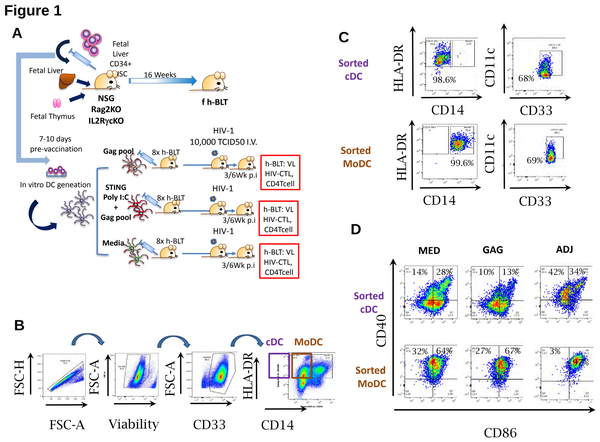


Figure 1. Generation of cDC and MoDC from human fetal liver HSC and vaccine design in the h-BLT mouse model (A): Schematic representation of the humanized BLT mouse experimental model. n=24 humanized BLT mice were generated using CD34+ HSC from the same precursors. A fraction of HSC were differentiated in the presence of FLT3L, SCF, IL-7 and GMCSF. Sorted DC were incubated with Media, Gag peptides and TBK-1 adjuvants and reinfused to n=8 hBLT mice (B-C): Flow cytometry sorting strategy identifying live CD33+ myeloid cells generated from HSC and including HLADR+ CD14- cDC and HLADR+ CD14+ MoDC-like cells prior (B) and after sorting (C). (D): Expression of CD40 and CD86 in sorted cDC and MoDC-like cells after 24h of culture in media (MED) or in the presence of Gag peptides alone (GAG) or in combination of TBK-1 adjuvants (ADJ).

Figure 2

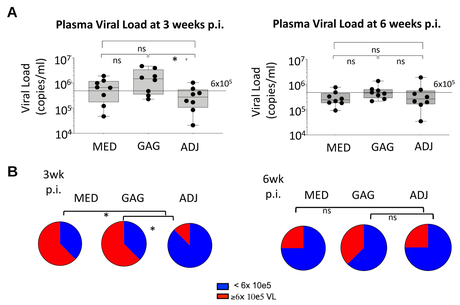


Figure 2. Plasma HIV-1 viral load in vaccinated humanized BLT-mice at 3 and 6 weeks post infection. (A): Plasma VLs measured by RT-qPCR from the plasma of hBLT-mice vaccinated with MED, GAG and GAG+ADJ (ADJ) treated DC at 3 (left panel) and 6 (right panel) weeks post infection. Significance was calculated using a two-tailed Mann Whitney test (*p<0.05) (B): Pie Charts illustrating proportions of mice with detectable viral loads lower (blue) and higher ´(red) than 6 x10e5 HIV-1 RNA copies/ml of plasma. Statistical significance of differences was calculated using a two-tailed Chi-square test (*; p<0.05).

Figure 3

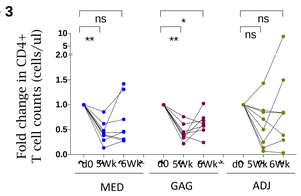


Figure 3. Depletion of CD4 T cells from the blood in infected hBLT mice. Fold change in CD4 T cell counts in the blood from hBLT mice vaccinated with DC treated with media (MED, blue), a pool of HIV-1 gag peptides (GAG) alone or in combination with TBK-1 adjuvants (ADJ) at 5 and 6 weeks post infection with HIV-1. Significance was calculated using a two-tailed Wilcoxon test (*p<0.05; **; p<0.01).

Figure 4

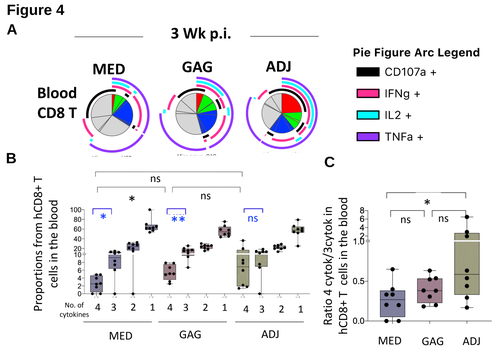


Figure 4. Cytokine polyfunctional profile in T cells from hBLT mice after infection with HIV-1. (A,C): Polyfunctional chary profiles observed in CD8+ T cells from the blood representing median values of cells co-expressing 4 (red), three (green), two (blue) or one (grey) of the indicated parameters (CD107a, IFNγ, IL-2, TNFa). Individual expression patterns of each parameters are represented in colored arcs as indicated by the legends. (B): Proportions of cells producing 4, 3, 2 and 1 cytokines within CD8+ T cells from the blood of the different humanized BLT mouse groups. Statistical significance in the distribution of proportions of different polyfunctional populations were calculated using a two-tailed Wilcoxon test within each group (blue) and a Mann Whitney test to compare among groups (black) (*, p<0.05; **, p<0.01). (C): Ratios of cells producing 4 vs 3 cytokines within circulating CD8+ T cells from the three indicated groups of mice. Statistical significance was calculated using a Mann Whitney test.

▪ However, a less dramatic and less significant depletion of CD4+ T cell lymphocytes was detected in the ADJ mice compared to the other two group of mice, suggesting delayed disease progression in animals vaccinated with DCs matured with TBK-1 adjuvants (**Figure 3**). At the immunological level, the group of mice vaccinated with GAG-ADJ DC were characterized by a higher polyfunctional profile with multiple cytokine expression in circulating CD8+ T cells at 3 weeks p.i., suggesting also partial control of viral replication at early time points (**Figure 4A**). These polyfunctional patterns were marked by a relative enrichment of CD8+ T cells co-expressing 4 cytokines at a time compared to populations with a lower level of polyfunctionality (**Figure 4B-4C**). Interestingly, while polyfunctionality contracted in the blood at 6 weeks p.i. in most animal groups, CD8 T cells expressing higher levels of TNFa and CD107a were observed in the ADJ group basally and after antigen stimulation (**Figure 5A**).

Figure 5

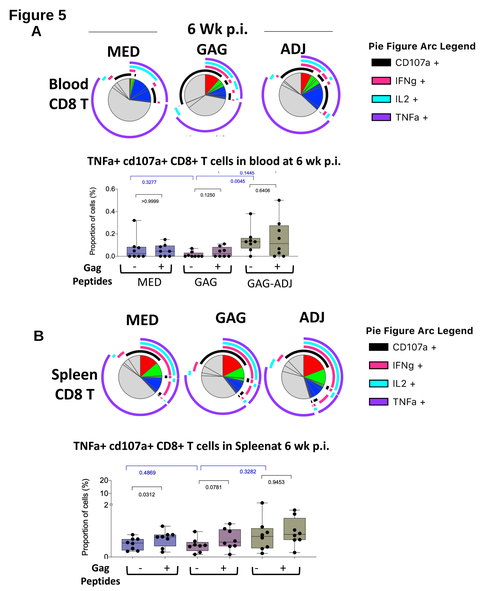


Figure 5. Cytokine polyfunctional profile in T cells from hBLT mice at 6 weeks after infection with HIV-1. (A,B upper panels): Polyfunctional chary profiles observed in CD8+ T cells from the blood (A) and spleen (B) representing median values of cells co-expressing 4 (red), three (green), two (blue) or one (grey) of the indicated parameters (CD107a, IFNγ, IL-2, TNFa). Individual expression patterns of each parameters are represented in coloured arcs as indicated by the legends. (A,B lower panels): Proportions of CD107a+ TNFa+ CD8+ T cells present in the blood (A) and spleen (B) from the trhee vaccinated mice groups. Statistical significance within or among mice groups was calculated using a two-tailed Wilcoxon test and a Mann Whitney test, respectively (*, p<0.05; **, p<0.01).

Figure 6

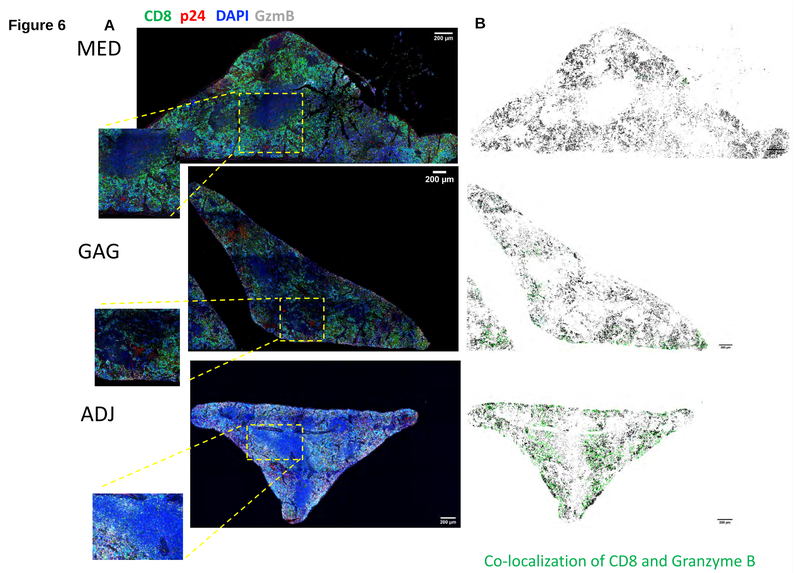


Figure 6. Histological analysis of CD8+ T cell, p24+ cells and granzyme B distribution on spleen from hBLT mice. (A): Representative immunofluorescence of a spleen section from MED, GAG and ADJ+GAG hBLT mice groups analyzing the distribution of CD8+ T cells (green), infected p24+ cells (red) and granzyme B+ cells (GzmB, grey) in different areas from the tissue. A magnification of highlighted areas is shown. (B): Image J analysis of co-localization of Granzyme B with CD8+ T cells from the same images shown in panel A. Cells co-expressing both markers are highlighted in green.

▪ In addition, we observed higher levels of polyfunctional CD8+ T cells in the spleens of all animals and a trend to superior proportions of CD107a+ TNFa+ CD8+ T cells in the ADJ-mice group. Immunofluorescence analysis of histological distribution of CD8 T cells in the spleen revealed higher proportions of infiltrated CD8+ T cells and proportions of cytotoxic Granzyme B+ cells in the ADJ mouse group compared to control animals. Interestingly, CD8+ T cells from ADJ mice tended to infiltrate within the spleen than in GAG and MED mice. Importantly, higher level of infiltration of CD8+ T cells and total cytotoxic Granzyme B+ cells seemed to be associated with early control of HIV viremia (**Figure 6, Figure 7A-7B**). Moreover, a higher proportion of CD8+ T cells co-expressing granzyme B in the ADJ animals was associated with higher CD4+ T cell counts, suggesting that preserved cytotoxic function of CD8+ T cells in these animals might contribute to delay disease progression in this model (**Figure 7C**).

Figure 7

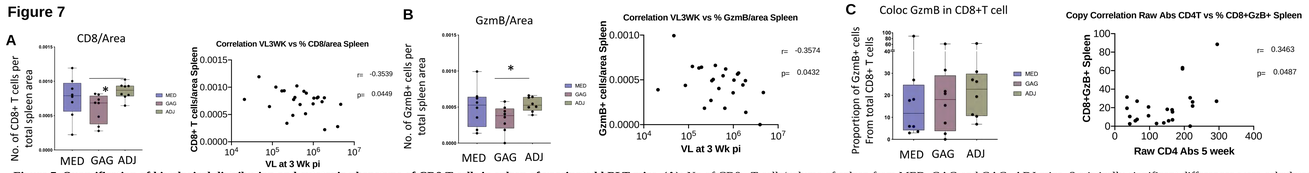


Figure 7. Quantification of histological distribution and cytotoxic phenotype of CD8 T cells in spleen of vaccinated hBLT-mice. (A): No of CD8+ T cells/volume of spleen from MED, GAG and GAG+ADJ mice. Statistically significant differences were calculated using a Mann Whitney test. *, p<0.05. Spearman correlation of CD8+T cells/area and plasma HIV-1 VL at 3 weeks post infection is shown. R and p values are shown on the right. (B): No of Granzyme B+ cells/volume of spleen from MED, GAG and GAG+ADJ mice. Statistically significant differences were calculated using a Mann Whitney test. *, p<0.05. Spearman correlation of Granzyme B+ cells/area and plasma HIV-1 VL at 3 weeks post infection is shown. R and p values are shown on the right. (C): Proportions of Granzime B+ cells included within splenic CD8+T cells. Spearman association between relative Granzyme B+ CD8+ T cells/area and raw CD4+ T cell counts in blood. R and p values are shown on the right.

▪ Moreover, we observed increased cluster volumes of CD8+ T cells in the lymph nodes from ADJ mice **(Figure 8)** while infected HIV-1 p24+ cells tended to be excluded from CD8+ T cell enriched areas within the node, and such exclusion was also associated with control of HIV viral load at early time points **(Figure 9).**

Figure 8

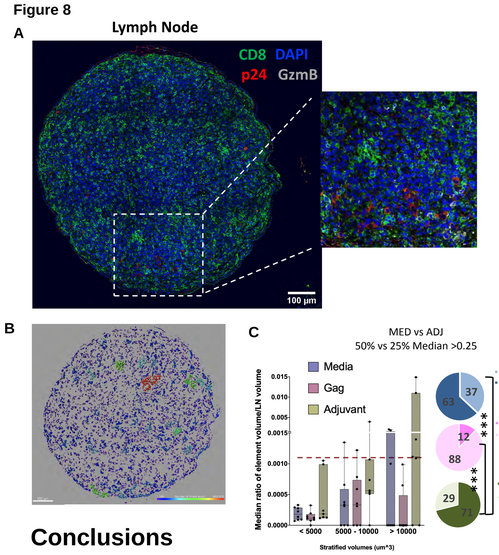


Figure 8. CD8+ T cell distribution in the lymph nodes of vaccinated hBLT-mice. (A): Representative confocal images of staining of lymph node tissue sections from hBLT mice vaccinated with DC treated with media (MED), a pool of gag peptides alone (GAG) or in combination with our TBK-1 adjuvants (ADJ) with DAPI (blue) and specific Abs against CD8 (green), HIV p24 (red) and Granzyme B (GzmB, Grey) as detailed in the panel and method section. (B): Representative image from an ADJ LN generated by Imaris software identifying different CD8 volume elements colored by different scales of volume defined as microns³ (C): Quantification of volume of CD8 clusters at 3 different ranges in the LNs from all group of animals relative to the total volume of each nodule. Statistical significance in distribution of proportions of CD8 T cell clusters with higher contribution to the tissue section volume is shown in pies on the right and calculated with a chi-square test.

Figure 9

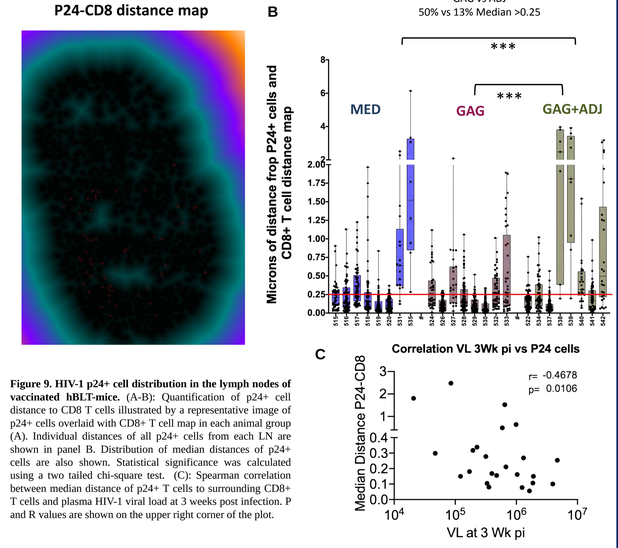


Figure 9. HIV-1 p24+ cell distribution in the lymph nodes of vaccinated hBLT-mice. (A-B): Quantification of p24+ cell distance to CD8 T cells illustrated by a representative image of p24+ cells overlaid with CD8+ T cell map in each animal group (A). Individual distances of all p24+ cells from each LN are shown in panel B. Distribution of median distances of p24+ cells are also shown. Statistical significance was calculated using a two tailed chi-square test. (C): Spearman correlation between median distance of p24+ T cells to surrounding CD8+ T cells and plasma HIV-1 viral load at 3 weeks post infection. P and R values are shown on the upper right corner of the plot.

Conclusions

▪ **Engineered TBK-1 DCs are able to induce polyfunctional CD8 T cells that are associated with improved clinical and histological parameters associated with immune control of HIV-1 infection in the hBLT-mouse model and might be useful for subsequent vaccine studies.**

Funding: We would like to thank the NIH R21 program (R21AI140930) Program for supporting these studies.